

Published in final edited form as:

*Neuroimage*. 2011 April 1; 55(3): 1068–1072. doi:10.1016/j.neuroimage.2010.11.086.

## Phase Contrast Imaging in Neonates

Kai Zhong<sup>1</sup>, Thomas Ernst<sup>2</sup>, Steve Buchthal<sup>2</sup>, Oliver Speck<sup>1</sup>, Lynn Anderson<sup>2</sup>, and Linda Chang<sup>2</sup>

<sup>1</sup>Department of Biomedical Magnetic Resonance, Faculty for Natural Sciences, Otto-von-Guericke University Magdeburg, Leipziger Strasse 44, Haus 65, D-39120, Magdeburg, Germany.

<sup>2</sup>Department of Medicine, JABSOM, University of Hawaii, 1356 Lusitana St., Honolulu, HI 96813, USA.

### Abstract

Magnetic resonance phase images can yield superior gray and white matter contrast compared to conventional magnitude images. However, the underlying contrast mechanisms are not yet fully understood. Previous studies have been limited to high field acquisitions in adult volunteers and patients. In this study, phase imaging in the neonatal brain is demonstrated for the first time. Compared to adults, phase differences between gray and white matter are significantly reduced but not inverted in neonates with little myelination and iron deposits in their brains. The remaining phase difference between the neonatal and adult brains may be due to different macromolecule concentration in the unmyelinated brain of the neonates and thus different frequency due to water macromolecule exchange. Additionally, the susceptibility contrast from brain myelination can be separately studied in neonates during brain development. Therefore, magnetic resonance phase imaging is suggested as a novel tool to study neonatal brain development and pathologies in neonates.

### Introduction

Recent studies at 7 Tesla field strength demonstrate that direct phase imaging can provide gray matter (GM) and white matter (WM) contrast with a contrast-to-noise ratio (CNR) that is an order of magnitude higher compared to conventional magnitude images (Duyn et al., 2007; Hammond et al., 2008; Zhong et al., 2008). The current understanding of the *in vivo* phase contrast involves two major contrast mechanisms, susceptibility (Duyn et al., 2007) and water-macromolecule exchange (WME) (Zhong et al., 2008). The susceptibility contrast contributions include para- or diamagnetic components, such as tissue iron content, blood hemoglobin, myelin content, tissue lipids, etc. The WME involves mostly mobile macromolecules in the cellular compartment. However, the contribution of each of these mechanisms to the total observed *in vivo* phase contrast is not fully understood and subject of ongoing investigations (He and Yablonskiy, 2009; Marques et al., 2009; Zhong et al., 2009).

© 2010 Elsevier Inc. All rights reserved.

**Corresponding author:** Kai Zhong, PhD Dept. of Biomedical Magnetic Resonance Otto-von-Guericke University Magdeburg Leipziger Strasse 44, Haus 65 D-39120, Magdeburg Germany Tel: +49 391 6117 116 Fax: +49 391 6117 115 kai.zhong@nat.uni-magdeburg.de.

**Publisher's Disclaimer:** This is a PDF file of an unedited manuscript that has been accepted for publication. As a service to our customers we are providing this early version of the manuscript. The manuscript will undergo copyediting, typesetting, and review of the resulting proof before it is published in its final citable form. Please note that during the production process errors may be discovered which could affect the content, and all legal disclaimers that apply to the journal pertain.

Many phase contrast studies were carried out at a field strengths of 7 Tesla or higher to take advantage of the superior signal-to-noise ratio (SNR) and frequency dispersion. All of these prior studies were performed on adult volunteers and patients or in small animals. In order to differentiate the various contributions to *in vivo* phase contrast in gray and white matter, isolation and quantification of individual components, such as myelin or macromolecule effects, are desired. However, this is impossible in the adult human brain since all contributing factors are present simultaneously.

In this study, phase imaging was performed in neonates. This offers the unique opportunity to evaluate the different contributions of unmyelinated versus myelinated brain tissue to the *in vivo* phase contrast in the human brain. It is well known that the neonatal brain structure and myelination changes rapidly during early development (Blackburn and Loper, 1992; Knickmeyer et al., 2008) leading to differences in brain tissue composition (Fountoulakis et al., 2000) compared to the adult brain. Previous MR studies focused on developmental changes in brain structure (Bartha et al., 2007; Knickmeyer et al., 2008),  $T_1$  and  $T_2$  relaxation times (Williams et al., 2005), brain metabolism (Bartha et al., 2007; Gilmore et al., 2004; Kim et al., 2006), and apparent water diffusion (Anjari et al., 2007; Bartha et al., 2007; Gilmore et al., 2004). These studies demonstrated marked differences between the neonate and adult brain, in particular with regards to reversed GM-WM contrast on  $T_1$  or  $T_2$ -weighted as well as diffusion weighted images (DWI). Additionally, the neonatal brain contains only small amounts of iron and myelin (Blackburn and Loper, 1992). Therefore, the neonatal brain provides an unique opportunity to investigate the different contributions of susceptibility and WME to phase contrast. More importantly, during normal neonatal brain development and the onset of myelination, the contribution from myelin can be evaluated. Therefore the purpose of this study is to perform phase imaging in neonatal brains and evaluate the potential of phase imaging as a novel approach to study brain development as well as neonatal pathologies.

## Methods

Experiments were carried out on a 3 Tesla (T) MR scanner (Siemens TIM Trio, Erlangen, Germany, 12-channel head coil) in 23 full-term neonates between 1 and 8 weeks of age. Informed written consents were provided by their parents prior to the experiments following the guidelines of the local institutional review board. Each neonate and their parents were carefully screened to ensure that they had no contraindications for the scans. The neonates were fed and allowed to fall asleep prior to the scan without sedation. Infant motion was minimized by wrapping the infants in a vacuum immobilization mat (Noras MRI Products, Hoechberg, Germany) with earplugs and earmuffs to protect hearing. The neonates were constantly monitored by an investigator during the duration of the scans. An RF-spoiled 2D gradient echo sequence was used to acquire the phase images, typically along axial orientation. Image acquisition parameters were:  $320 \times 288$  matrix size with  $0.5 \times 0.5$  mm<sup>2</sup> in-plane resolution; TR/TE = 980/35 ms; flip angle = 50°; 20 slices, slice thickness 2 mm. In addition, 3D-MPRAGE (Magnetization Prepared Rapid Acquisition Gradient Echo) images ( $256 \times 256 \times 160$ , 1 mm<sup>3</sup> isotropic resolution, TR/TE = 2500/3.98 ms, TI = 1100 ms) were acquired in sagittal orientation. MATLAB (Natick, USA) and SPM5 (Wellcome Trust Centre for Neuroimaging, London, UK; [www.fil.ion.ucl.ac.uk/spm](http://www.fil.ion.ucl.ac.uk/spm)) were used for data processing, extended by in house software developed for phase data reconstruction.

Our experiment, similar to many previous direct phase imaging studies, adapted anisotropic voxels, e.g. higher in-plane resolution (0.5 mm) and thicker slice thickness (2 mm). Although such anisotropic acquisition method does improve visually the brain tissue contrast, it might introduce potential problems relating to partial volume effect.

MPRAGE images were used for guiding locations of early myelination and coregistered with the GRE images, using SPM5 software. Problems did occur occasionally for some datasets, which might be due to different image contrast in neonatal GRE and MPRAGE images. We suggest that an improved neonate brain template could help the alignment procedure. Phase images were selected based on motion artifacts presented clearly along the phase encoding direction (R-L). If the ghost artifact was above 5% of the mean GM/WM intensity, head motion was considered to be too strong and the corresponding dataset was rejected from the final analysis. A combination algorithm based on the SENSE reconstruction (Pruessmann et al., 1999) was used to obtain the phase images from the complex single channel datasets. The sensitivity profile of each individual RF receiver channel was created by low-pass filtering the corresponding complex data. An optimal filter size of 2.5 mm was applied (Yang et al., 2009). Final phase images were created by SENSE reconstruction with an acceleration factor of 1. This procedure also removes the field inhomogeneity artifacts without the requirement of further high-pass filtering the resulting phase images. On the other hand, high-pass filtering the phase data could also partially increase the local correlation between voxels. Brain masks were created from the magnitude images and were applied to the phase images to remove skull tissue signals.

The GM-WM phase separations were determined in four brain regions (occipital lobe, parietal lobe, frontal cortex and thalamus). For each region, two carefully selected regions of interest (ROIs) in GM and WM from GRE phase images that were void of observable vessels were used to determine the phase difference. Due to strong variation in local demagnetization field in different brain regions, absolute phase quantitation across different brain regions is currently unavailable. Therefore, GM/WM phase separation can only be reliably determined between locally adjacent tissue types. The GM and WM ROIs were from adjacent locations determined from the GRE images as well as the MPRAGE images in different brain regions and were matched as closely as possible between subjects. In addition, regions of early myelination in the internal capsule were compared to surrounding WM regions that showed no myelination in the  $T_1$ -weighted images to estimate the phase contrast from early brain myelination. All phase shifts are reported in units of parts per million (ppm).

## Results

Since no sedation was used in the study, head motion constituted a major problem despite immobilization measures. Only in 7 (5 boys, 2 girls) out of 23 neonates had satisfactory phase images, corresponding to a success rate of 30%. Phase images were selected based on motion artifacts presented clearly along the phase encoding directions and images with strong head motion were rejected from the final analysis.

A typical magnitude gradient echo (GRE) image from a 28-day old neonate (postconceptional age 42 weeks) is shown in Figure 1a, with the corresponding phase image in Figure 1b. The MP-RAGE image from the same subject is shown in Figure 1c and 1d. In both the GRE and MPRAGE images, reversed GM-WM contrast can be observed with respect to the adult brain. This suggests a shorter  $T_2^*$  and  $T_1$  for GM compared to WM, consistent with literature results. In this neonate, myelination can be observed in the internal capsule, depicted by the higher signal intensity in the MPRAGE images in both the axial and sagittal views.

The neonate phase images show positive phase in GM compared to the surrounding WM, which is similar to results from studies in adults (Duyn et al., 2007; Hammond et al., 2008; Zhong et al., 2008). Although phase contrast in the neonatal brain is overall smaller, it is still possible to quantify the GM-WM phase difference. The GM-WM phase difference values in

several brain regions (occipital lobe, frontal lobe, parietal lobe, and thalamus) are shown in Table 1. The phase difference showed little variation among brain regions, with an average phase difference of 0.0035 ppm. Additionally, the WM region where myelin has begun formation, noticeably in the internal capsule, was also selected and compared to the surrounding WM regions without myelination, as shown in Figure 2b. The estimated phase difference between these regions is -0.0036 ppm. The experimental observations were consistent across all seven neonatal data sets that were evaluated (Table 1).

Additionally, adult phase images with matched acquisition parameters were acquired in three healthy adult control subjects at 3 T (Figure 3). The images showed much stronger phase contrast between GM and WM than the neonates, with an estimated average GM-WM phase separation of approximately 0.01 ppm (occipital lobe).

## Discussion

To our knowledge, this is the first study of phase contrast MRI in neonates. The results demonstrate that the phase shift is stronger in GM than in WM. While the other MR-contrasts, such as  $T_1$ ,  $T_2$ , and  $T_2^*$ , are inverted in the neonates compared to those in the adult brain, the direction of phase contrast is the same as in adults. However, adults show larger GM to WM contrast of up to 0.01 ppm at 3 T, compared to 0.0035 ppm in the neonatal brain. Therefore, GM-WM phase contrast in the neonatal brain is approximately 60% smaller than that in the adult brain. Despite the reduced GM-WM neonatal phase contrast at 3 T, the phase contrast between GM-WM can still be resolved in these neonates.

One of the main differences between adult and neonate MR images is the reversal of  $T_1$ ,  $T_2$  and apparent diffusion coefficient (ADC) between GM and WM. If the mechanisms underlying this reversal also drive phase contrast, then one would hypothesize reversed phase contrast in neonates compared to adults as well. However, our experimental observations are inconsistent with this hypothesis. Therefore, we will discuss the potential contributions from both susceptibility and WME in phase contrast of the neonatal brain compared to that in the adult brain.

### Susceptibility contributions in the neonatal brain

The human neonatal brain contains little iron and virtually no myelin in most brain regions (Blackburn and Loper, 1992). In addition, studies of iron depositions in the neonatal rat brain suggested a highly localized distribution of iron, mostly in WM (Cheepsunthorn et al., 1998; Connor et al., 1995). Therefore, the major sources for susceptibility phase contrast in the neonatal brain are blood hemoglobin, macromolecules, and iron in WM. A recent phase imaging study in rats performed at 14.1 T (Marques et al., 2009) suggested that the blood hemoglobin contribution to total GM-WM phase contrast can be largely neglected. Since the rat study was carried out with an in-plane resolution of 0.033 mm, the authors suggested that lower image resolution may introduce large vessel contributions and increase the observed GM-WM contrast. However, an earlier functional MRI (fMRI) phase contrast study (Zhong et al., 2007) suggested a phase shift of 0.0026 ppm in GM relative to WM measured at 7 T. Since the resolution used in the earlier fMRI study (2mm) was inferior to that of the current study (0.5 mm), 0.0026 ppm can be assumed to be an upper limit for the GM-WM phase contrast due to hemoglobin from veins as observed at 3 T. Therefore, it is unlikely that the blood hemoglobin contribution alone can account for the *in vivo* GM-WM phase contrast in the neonates.

Macromolecules also create a susceptibility contribution to the total phase contrast, albeit negative (diamagnetic) compared to tissue iron (paramagnetic). Early Computer Tomography (CT) studies in neonates suggested higher macromolecule content in GM

compared to WM (Brant-Zawadzki and Enzmann, 1981). If a diamagnetic macromolecule contribution were the dominant effect, one would expect a negative phase contrast in GM compared to WM. Such an assumption would be demonstrated by a reversed GM-WM phase contrast compared to that seen in adult brains, similar to the inverted  $T_1$ ,  $T_2$ , and DWI contrasts in the neonates. However, this reversed GM-WM phase contrast is not observed in our neonates in this study.

Although iron is present in lower concentration in neonates than in adults, it could still contribute to the total GM-WM contrast. On the other hand, the iron distribution in the neonatal brain is heterogeneous and localized mostly in the WM (Cheepsunthorn et al., 1998; Sipe et al., 2002). Therefore, if tissue iron contributed substantially to the GM-WM phase contrast in neonates, again, a more negative phase in GM would be expected, which is opposite to our experimental observations.

Therefore, one can conclude that susceptibility related phase shifts are unlikely to be the major contribution to the GM-WM phase contrast in the neonatal brains. Interestingly, a negative phase shift, most likely originating from diamagnetic myelin, is observed in the internal capsule where myelination is clearly visible on MRI at the postconceptional age of 42 weeks. Since iron is also co-localized in the brain WM, this negative phase shift following myelination suggests that myelin is the major susceptibility contribution to total GM-WM phase contrast in the neonates following brain myelination processes.

### WME contribution in the neonate brain

The high level of macromolecules in neonatal GM detected in a CT study is consistent with recent MR DTI findings (Anjari et al., 2007; Bartha et al., 2007; Gilmore et al., 2004) of lower water diffusion coefficients in GM compared to WM, probably since macromolecules tend to reduce the diffusion coefficient of water molecules. In addition, the reversed  $T_1$  and  $T_2$  contrasts in the neonates can also be explained by the high macromolecule concentration in GM, which reduces both water  $T_1$  and  $T_2$  values. Unfortunately, no studies on macromolecule concentration in neonates using MR spectroscopy have been published.

Measurements of macromolecule and lipid concentrations in the rat brain have been reported (Reddy and Horrocks, 1982) which demonstrate that proteins are the dominant component in both GM and WM (60 - 70 %). For neonates, the cholesterol and phosphorus lipid levels are expected to be similar for GM and WM prior to myelination. Reported data on water fractions in neonatal GM and WM are 87% and 89% respectively (van der Knaap and Valk, 2005). Therefore, the 2% difference most likely reflects the GM-WM protein difference, which is close to 14 mg/g.

The WME shift depends on the molecular size of the macromolecules and can be estimated by the molecular weight (Mw) distribution in tissue, as determined by chromatographic separation of the cytosolic macromolecule fraction (Behar and Ogino, 1993). 80 - 90 % of the mobile macromolecules are distributed within the 25 ~ 150 kDa range in the brain cytosol. This coincides with bovine serum albumin (BSA), which has a Mw of 67 kDa and a WME shift of 0.04 ppm/mM (Zhong et al., 2008). Therefore, we estimate that the WME shift due to macromolecules is about half compared to that from BSA only, based on the WME shift dependency on macromolecule size (Zhong et al., 2009). For a GM-WM difference of 14 mg in protein content, the corresponding WME frequency shift is estimated as 0.004 ppm. This result is consistent with the observed 0.0035 ppm GM-WM phase separation in neonates and suggests that the WME effect is a significant if not the dominant contributor to the neonatal *in vivo* GM-WM phase contrast.

Several recent publications suggest that the *in vivo* phase contrast in adult brains originates mainly from tissue susceptibility (He and Yablonskiy, 2009; Schaefer et al., 2009). Our phase study of neonatal brains suggests that the WME phase contrast is smaller compared to susceptibility effect seen in adult brains and does not contradict with the susceptibility model. However, the likely dominance of WME in neonates suggests that the WME contrast mechanism can not be omitted in any demagnetization model that evaluates the susceptibility contributions to *in vivo* phase contrast. Based on the current study, it can be estimated that the WME contribution is 2 – 3 times smaller compared to susceptibility contributions. This result therefore will help to refine the susceptibility model for *in vivo* phase contrast analysis. The smaller WME effect is also supported by observations in an adult rat study performed at 14.1 T (Marques et al., 2009).

The smaller phase separation (-0.0036 ppm) in myelinated WM areas at the postconceptional age of 42 weeks compared to 0.01 ppm in adult brain suggests partial myelination in the neonate WM. Therefore, the phase imaging method may offer a potentially more direct approach to study the brain myelination processes, in addition to the established methods that exploit the  $T_1$ ,  $T_2$ , water density and diffusion effects in WM. Comparison between  $T_2^*$  and  $T_1$  maps with phase contrast will be highly interesting to relate phase differences with differences in  $T_2^*$  and  $T_1$ . On the other hand, systematic studies are required to derive this important information and can be performed in future studies. Our results suggest that myelin is another important and dynamic source of phase contrast in the neonates. It is an interesting open question to what extent brain iron contributes to the neonatal phase contrast, especially during early neonatal brain development. Systematic investigation comparing neonate and adults would allow for additional hypothesis test on the effect of iron or myelin. Such effects require longitudinal data that could be obtained in potential future studies, which is beyond the scope of this paper. On the other hand, this study suggests that phase imaging can be applied to investigate brain development in neonates and related neonatal brain pathologies.

## Conclusion

This first study of phase contrast in the neonatal brain suggests that several contributing factors, such as water macromolecule exchange and myelination, can be separated. The WME most likely dominates early neonatal brain phase contrast and is estimated to contribute about 35% to the contrast typically seen in the adult phase images. Contributions from myelin also may show an age-dependent change. Therefore, phase imaging is a useful and complementary method to study early brain development and related pathologies that involve macromolecular alterations or brain myelination changes.

## Acknowledgments

This study is supported by the European Union sponsored CBBS NeuroNetwork Project (KZ), the National Institutes of Neurological Disorders and Strokes, and the National Institutes on Drug Abuse (1U54 NS056883-01, 2K24 DA016170 for LC; K02DA016991 for TE), with infrastructure support from the National Center for Research Resources (G12RR003061-21, RCMI and 5P20 RR11091-10 for the RCMI-CRC).

## References

- Anjari M, Srinivasan L, Allsop JM, Hajnal JV, Rutherford MA, Edwards AD, Counsell SJ. Diffusion tensor imaging with tract-based spatial statistics reveals local white matter abnormalities in preterm infants. *Neuroimage*. 2007; 35:1021–1027. [PubMed: 17344066]
- Bartha AL, Yap KRL, Miller SP, Jeremy RJ, Nishimoto M, Vigneron DB, Barkovich AJ, Ferriero DM. The normal neonatal brain: MR imaging, diffusion tensor imaging, and 3D MR spectroscopy

- in healthy term neonates. *American Journal of Neuroradiology*. 2007; 28:1015–1021. [PubMed: 17569948]
- Behar KL, Ogino T. Characterization of macromolecule resonances in the <sup>1</sup>H NMR spectrum of rat brain. *Magn Reson Med*. 1993; 30:38–44. [PubMed: 8371672]
- Blackburn, ST.; Loper, DL. *Maternal, fetal and neonatal physiology: a clinical perspective*. W.B. Saunders; Philadelphia, PA: 1992.
- Brant-Zawadzki M, Enzmann DR. Using computed tomography of the brain to correlate low white-matter attenuation with early gestational age in neonates. *Radiology*. 1981; 139:105–108. [PubMed: 7208910]
- Cheepsunthorn P, Palmer C, Connor JR. Cellular distribution of ferritin subunits in postnatal rat brain. *J Comp Neurol*. 1998; 400:73–86. [PubMed: 9762867]
- Connor JR, Pavlick G, Karli D, Menzies SL, Palmer C. A histochemical study of iron-positive cells in the developing rat brain. *J Comp Neurol*. 1995; 355:111–123. [PubMed: 7636007]
- Duyn JH, van Gelderen P, Li TQ, de Zwart JA, Koretsky AP, Fukunaga M. High-field MRI of brain cortical substructure based on signal phase. *Proceedings of the National Academy of Sciences of the United States of America*. 2007; 104:11796–11801. [PubMed: 17586684]
- Fountoulakis M, Hardmaier R, Schuller E, Lubec G. Differences in protein level between neonatal and adult brain. *Electrophoresis*. 2000; 21:673–678. [PubMed: 10726776]
- Gilmore JH, Zhai GH, Wilber K, Smith JK, Lin WL, Gerig G. 3 Tesla magnetic resonance imaging of the brain in newborns. *Psychiatry Research-Neuroimaging*. 2004; 132:81–85.
- Hammond KE, Lupo JM, Xu D, Metcalf M, Kelley DA, Pelletier D, Chang SM, Mukherjee P, Vigneron DB, Nelson SJ. Development of a robust method for generating 7.0 T multichannel phase images of the brain with application to normal volunteers and patients with neurological diseases. *Neuroimage*. 2008; 39:1682–1692. [PubMed: 18096412]
- He X, Yablonskiy DA. Biophysical mechanisms of phase contrast in gradient echo MRI. *Proceedings of the National Academy of Sciences*. 2009; 106:13558–13563.
- Kim DH, Barkovich AJ, Vigneron DB. Short Echo Time MR Spectroscopic Imaging for Neonatal Pediatric Imaging. *American Journal of Neuroradiology*. 2006; 27:1370–1372. [PubMed: 16775299]
- Knickmeyer RC, Gouttard S, Kang CY, Evans D, Wilber K, Smith JK, Hamer RM, Lin W, Gerig G, Gilmore JH. A Structural MRI Study of Human Brain Development from Birth to 2 Years. *Journal of Neuroscience*. 2008; 28:12176–12182. [PubMed: 19020011]
- Marques JP, Maddage R, Mlynarik V, Gruetter R. On the origin of the MR image phase contrast: an in vivo MR microscopy study of the rat brain at 14.1 T. *Neuroimage*. 2009; 46:345–352. [PubMed: 19254768]
- Pruessmann KP, Weiger M, Scheidegger MB, Boesiger P. SENSE: sensitivity encoding for fast MRI. *Magn Reson Med*. 1999; 42:952–962. [PubMed: 10542355]
- Reddy TS, Horrocks LA. Effects of neonatal undernutrition on the lipid composition of gray matter and white matter in rat brain. *J Neurochem*. 1982; 38:601–605. [PubMed: 7199078]
- Schaefer A, Wharton S, Gowland P, Bowtell R. Using magnetic field simulation to study susceptibility-related phase contrast in gradient echo MRI. *Neuroimage*. 2009; 48:126–137. [PubMed: 19520176]
- Sipe JC, Lee P, Beutler E. Brain Iron Metabolism and Neurodegenerative Disorders. *Developmental Neuroscience*. 2002; 24:188–196. [PubMed: 12401958]
- van der Knaap, MS.; Valk, J. *Magnetic Resonance of Myelination and Myelin Disorders*. Springer; New York: 2005.
- Williams L-A, Gelman N, Picot PA, Lee DS, Ewing JR, Han VK, Thompson RT. Neonatal Brain: Regional Variability of in Vivo MR Imaging Relaxation Rates at 3.0 T--Initial Experience. *Radiology*. 2005; 235:595–603. [PubMed: 15858099]
- Yang S, Zhong K, Grinstead J, Speck O. Optimal Combination and Filtering for 7 T – Phase Images. *Proc. Intl. Soc. Mag. Reson. Med*. 2009; 17:4574.
- Zhong K, Leupold J, Stadler J, Tempelmann C, Speck O. Phase fMRI at 7 Tesla. *Proc. Intl. Soc. Mag. Reson. Med*. 2007; 15:3197.

- Zhong K, Leupold J, von Elverfeldt D, Speck O. The molecular basis for gray and white matter contrast in phase imaging. *Neuroimage*. 2008; 40:1561–1566. [PubMed: 18353683]
- Zhong K, Smalla K-H, Brensing A, Speck O. Molecular Size Dependency of Water Macromolecule Exchange Induced Frequency Shift. *Proc. Intl. Soc. Mag. Reson. Med.* 2009; 17:864.



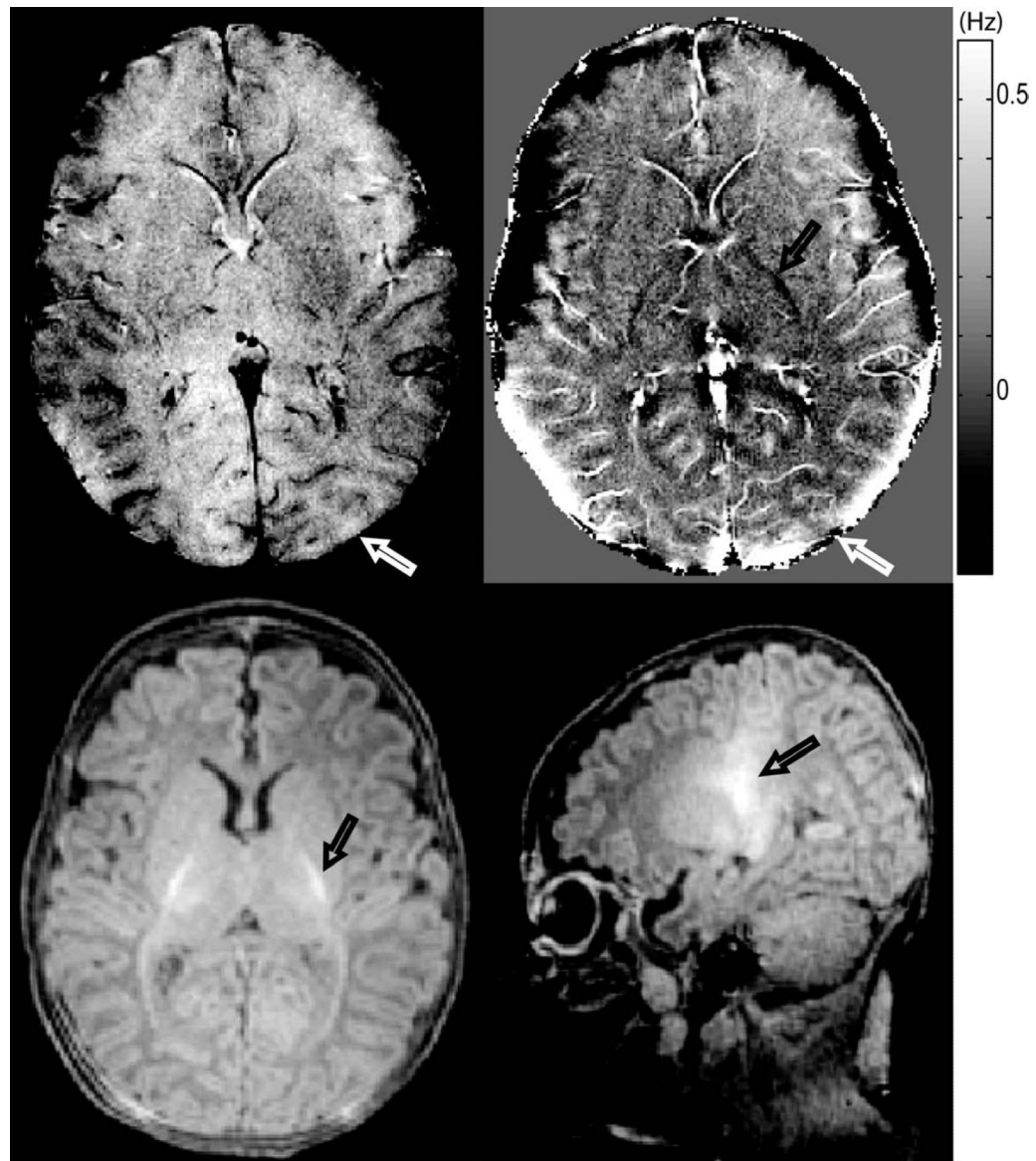


**Figure 1. Phase contrast in a neonatal brain at 3 Tesla**

a) 2D GRE image with a resolution of  $0.5 \times 0.5 \text{ mm}^2$ ; b) corresponding phase images; c) and d) T<sub>1</sub>-weighted MPRAGE images in axial and sagittal views depicting the locations of myelination (long arrow). White arrows point to locations of GM-WM phase contrast that showed reverse contrast in T<sub>2</sub>\* and T<sub>1</sub> images. Black arrows point to locations of myelination in internal capsule at 42 weeks postconceptional age.

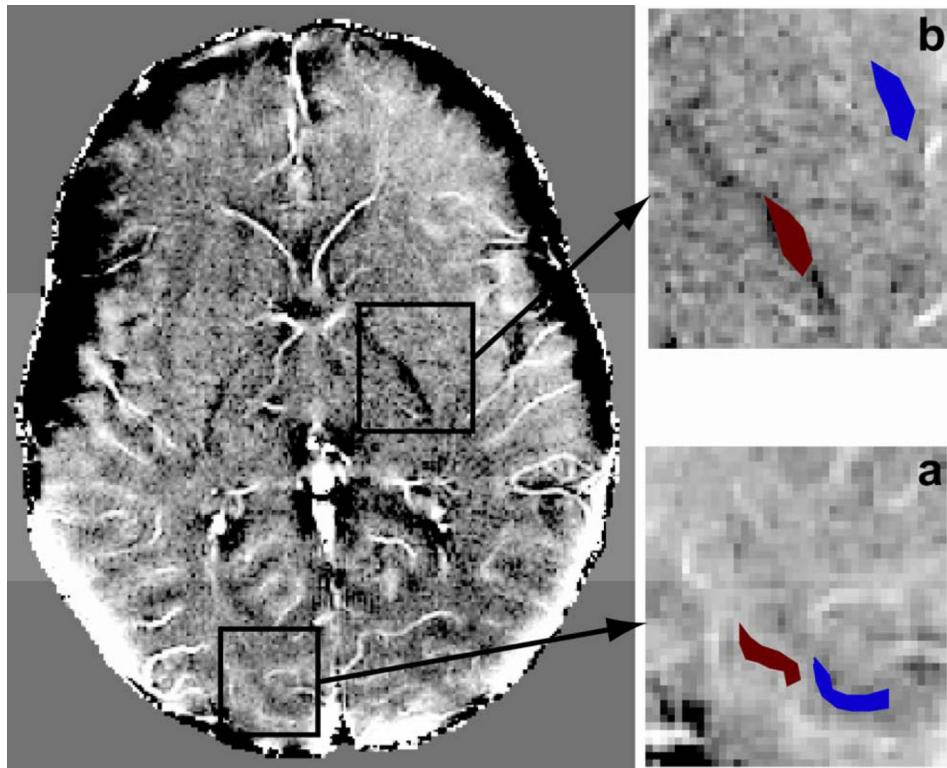


**Figure 2. The GM-WM phase separation in the brains of neonates at 3 T**

The GM-WM phase separation is determined in selected ROIs (a). GM (red) and WM (blue) regions without large veins are selected. The average GM-WM separation is 0.0035 ppm. b) Selected regions in WM with (red) and without (blue) myelination in internal capsule are used to determinate the phase shift related to myelination in WM (-0.0036 ppm).

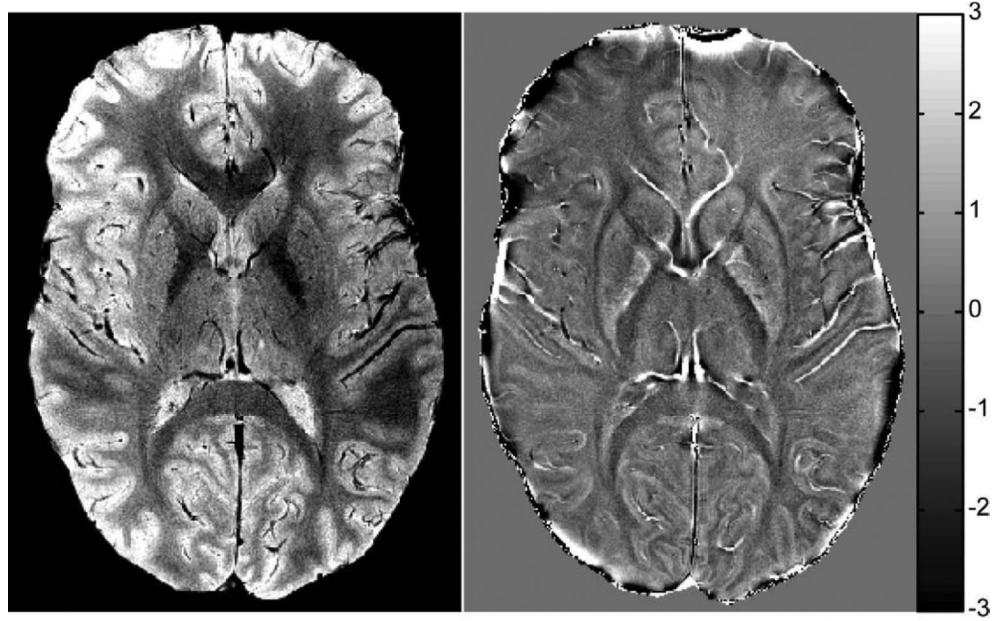


**Figure 3. Phase contrast in an adult brain at 3T**

Images were acquired with the same methods as those in the neonates. The phase image shows a much stronger contrast compared to that in the neonates. Both negative phase shift in the internal capsule due to myelin and positive phase shift due to iron in the thalamus are observed.

**Table 1**

Phase separation (in ppm) between GM and WM in selected brain regions.

Brain regions	Subject 1	Subject 2	Subject 3	Subject 4	Subject 5	Subject 6	Subject 7	Average
Occipital lobe	0.0039	0.0037	0.0036	0.0033	0.0037	0.0033	0.0036	0.0035 ± 0.0003
Frontal cortex	0.0036	0.0035	0.0034	0.0042	0.0029	0.0034	0.0031	0.0034 ± 0.0004
Parietal lobe	0.0041	0.0040	0.0037	0.0036	0.0037	0.0032	0.0032	0.0036 ± 0.0004
Thalamus	0.0037	0.0036	0.0040	0.0031	0.0031	0.0030	0.0030	0.0034 ± 0.0004
Internal capsule*	-0.0035	-0.0030	-0.0038	-0.0034	-0.0037	-0.0034	-0.0036	-0.0036±0.0004

Four different brain regions (occipital lobe, parietal lobe, frontal cortex and thalamus) were selected. The average GM-WM phase separation was 0.0035 ppm.

\* Phase separation from WM myelination in the internal capsule was -0.0036 ppm.